



ASCT1 (Slc1a4) transporter is a physiologic regulator of brain D-serine and neurodevelopment

Eitan Kaplan^a, Salman Zubedat^b, Inna Radzishevsky^a, Alec C. Valenta^c, Ohad Rechnitz^d, Hagit Sason^a, Clara Sajrawi^a, Oded Bodner^a, Kohtarou Konno^e, Kayoko Esaki^f, Dori Derdikman^d, Takeo Yoshikawa^f, Masahiko Watanabe^e, Robert T. Kennedy^c, Jean-Marie Billard^{g,h,1}, Avi Avital^{b,1}, and Herman Wolosker^{a,1}

^aDepartment of Biochemistry, Rappaport Faculty of Medicine, Technion – Israel Institute of Technology, 31096 Haifa, Israel; ^bDepartment of Physiology, Rappaport Faculty of Medicine, Technion – Israel Institute of Technology, 31096 Haifa, Israel; ^cDepartment of Chemistry, University of Michigan, Ann Arbor, MI 48109; ^dDepartment of Neurosciences, Rappaport Faculty of Medicine, Technion – Israel Institute of Technology, 31096 Haifa, Israel; ^eDepartment of Anatomy, School of Medicine, Hokkaido University, 060-8638 Sapporo, Japan; ^fLaboratory for Molecular Psychiatry, RIKEN Brain Science Institute, Wako, 351-0198 Saitama, Japan; ^gCenter of Psychiatry and Neuroscience, UMR 894, University Paris Descartes, 75014 Paris, France; and ^hU1075 INSERM, Université de Caen Normandie, 14032 Caen cedex 5, France

Edited by Robert H. Edwards, University of California, San Francisco, CA, and approved August 13, 2018 (received for review January 1, 2018)

D-serine is a physiologic coagonist of NMDA receptors, but little is known about the regulation of its synthesis and synaptic turnover. The amino acid exchangers ASCT1 (Slc1a4) and ASCT2 (Slc1a5) are candidates for regulating D-serine levels. Using ASCT1 and ASCT2 KO mice, we report that ASCT1, rather than ASCT2, is a physiologic regulator of D-serine metabolism. ASCT1 is a major D-serine uptake system in astrocytes and can also export L-serine via heteroexchange, supplying neurons with the substrate for D-serine synthesis. ASCT1-KO mice display lower levels of brain D-serine along with higher levels of L-alanine, L-threonine, and glycine. Deletion of ASCT1 was associated with neurodevelopmental alterations including lower hippocampal and striatal volumes and changes in the expression of neurodevelopmental-relevant genes. Furthermore, ASCT1-KO mice exhibited deficits in motor function, spatial learning, and affective behavior, along with changes in the relative contributions of D-serine vs. glycine in mediating NMDA receptor activity. In vivo microdialysis demonstrated lower levels of extracellular D-serine in ASCT1-KO mice, confirming altered D-serine metabolism. These alterations are reminiscent of some of the neurodevelopmental phenotypes exhibited by patients with ASCT1 mutations. ASCT1-KO mice provide a useful model for potential therapeutic interventions aimed at correcting the metabolic impairments in patients with ASCT1 mutations.

slc1a4 | D-serine | ASCT1 | Slc1a5 | glycine

NMDA receptors (NMDARs) play key roles in neurodevelopment, synaptic plasticity, and learning and memory (1). Unlike other neurotransmitter receptors, the NMDARs require the binding of a coagonist (D-serine or glycine) in addition to glutamate (1). D-serine is synthesized from L-serine by the serine racemase (SR) (2). SR-KO mice display a 90% decrease in brain D-serine and exhibit impairments in NMDAR-dependent synaptic plasticity (3–5). However, the mechanisms regulating D-serine metabolism in the forebrain remain unknown. Early studies reported exclusive astrocytic localizations of D-serine (6), leading to the suggestion that D-serine is a gliotransmitter. However, recent studies using more selective antibodies and SR-KO as controls indicate that SR is predominantly expressed by neurons (7–9). In agreement, selective deletion of SR from neurons decreases the synaptic plasticity at the Schaffer collateral-CA1 hippocampal synapses both in vitro and in vivo (5, 9).

Brain L-serine is synthesized from glucose by a series of enzymes that include 3-phosphoglycerate dehydrogenase (3PGDH), which is exclusively expressed in astroglia. Astrocyte-selective deletion of 3PGDH in mice strongly decreases the levels of neuronal D-serine (8). These data led us to propose an astrocyte–neuron metabolic cross-talk called the serine shuttle, whereby L-serine synthesized in astrocytes shuttles to neurons and fuels the synthesis of D-serine (10).

The alanine, serine, cysteine, and threonine exchangers ASCT1 (SLC1a4) and ASCT2 (SLC1a5) transport D-serine in transfected HEK293 cells (11). ASCT2 has a broader substrate selectivity, acting on glutamine as well (12). However, their relevance in transporting D-serine or other brain amino acids in vivo has not been evaluated.

To identify the L- and D-serine transporters in astrocytes and study their role in vivo, we investigated ASCT1-KO and ASCT2-KO mice. We found that ASCT1, rather than ASCT2, is a component of the brain serine shuttle. ASCT1-KO mice display motor and neurodevelopmental deficits reminiscent of ASCT1 missense mutations in humans. The data indicate a role of ASCT1 in astroglia–neuron metabolic cross-talk and neurodevelopment.

Results

Role of ASCT1 and ASCT2 in Amino Acid Transport. We established ASCT1-KO and ASCT2-KO mice colonies and studied their role in brain amino acid transport. ASCT1-KO and ASCT2-KO

Significance

D-serine regulates synaptic plasticity and behavior by binding to the NMDA receptors. Astrocyte–neuron cross-talk provides L-serine for the synthesis of D-serine in a process called the serine shuttle. We show that the neutral amino acid antiporter ASCT1 can release L-serine from astrocytes in exchange for D-serine and other amino acid substrates. Mice lacking ASCT1, but not the paralogue ASCT2, display altered brain levels of L-serine, D-serine, L-alanine, L-threonine, and glycine. Deletion of ASCT1 was associated with decreased volume of different brain regions, altered gene expression, and motor and learning deficits. Our study sheds light on the role of ASCT1 in brain metabolism, with implications for the pathophysiology of the neurodevelopmental impairments observed in patients with mutations in the ASCT1 gene.

Author contributions: H.W. conceived the project; D.D., J.-M.B., A.A., and H.W. designed research; E.K., S.Z., I.R., A.C.V., O.R., H.S., C.S., K.K., K.E., M.W., J.-M.B., A.A., and H.W. performed research; O.B., K.E., T.Y., and R.T.K. contributed new reagents/analytic tools; E.K., S.Z., I.R., A.C.V., O.R., H.S., C.S., D.D., T.Y., M.W., R.T.K., J.-M.B., A.A., and H.W. analyzed data; and H.W. wrote the paper.

The authors declare no conflict of interest.

This article is a PNAS Direct Submission.

Published under the PNAS license.

Data deposition: The data reported in this paper have been deposited in the Gene Expression Omnibus (GEO) database, <https://www.ncbi.nlm.nih.gov/geo> (accession no. GSE108675).

¹To whom correspondence may be addressed. Email: jean-marie.billard@inserm.fr, avital@technion.ac.il, or hwolosker@tx.technion.ac.il.

This article contains supporting information online at www.pnas.org/lookup/suppl/doi:10.1073/pnas.1722677115/-DCSupplemental.

Published online September 5, 2018.

homozygotes are viable and fertile. ASCT1-KO mice had no detectable ASCT1 protein in the brain (*SI Appendix, Fig. S1*). Since the expression of ASCT2 in the brain is below the affinity of our antibody, we confirmed the lack of ASCT2 critical exons in the brain of ASCT2-KO mice by PCR, along with lack of protein expression in the kidneys, where ASCT2 is highly expressed (*SI Appendix, Fig. S1*).

We observed an 80–90% decrease in the transport of D-serine and L-serine in cultured astrocytes from ASCT1-KO mice (Fig. 1 *A* and *B*). Transport of typical ASCT1 substrates (e.g., L-alanine and L-threonine) was also significantly decreased (Fig. 1 *C* and *D*). In addition, glycine transport by ASCT1-KO astrocytes was 40% lower than WT (Fig. 1*E*), while glutamate uptake was unaffected (Fig. 1*F*).

Under physiological conditions, other extracellular amino acid substrates may bind with high affinity to ASCT1 and prevent D-serine transport. Therefore, we tested the uptake of D-[³H]serine in the presence of typical extracellular concentrations of ASCT1 substrates [14 μM L-alanine, 36 μM L-serine, 2 μM L-cysteine, and 18 μM L-threonine (13)]. Under these conditions, ASCT1 still transported D-serine (Fig. 1*G*). In contrast, no ASCT1-dependent uptake of glycine was detectable in the presence of the other ASCT1 substrates (Fig. 1*H*), suggesting glycine is a poor ASCT1 substrate.

However, the uptake of D-serine, L-serine, L-glutamine, and L-glutamate was unaltered in primary astrocyte cultures of ASCT2-KO mice (Fig. 1 *I–L*).

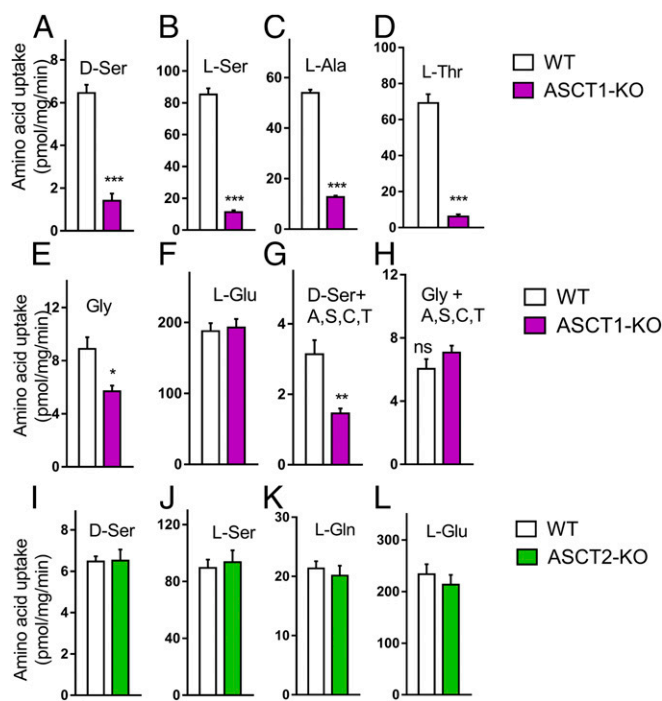


Fig. 1. Amino acid transport by astroglia of ASCT1-KO and ASCT2-KO mice. (*A–H*) Amino acid uptake in primary astrocyte cultures from WT and ASCT1-KO mice carried out in HEPES-buffered saline solution (HBSS) supplemented with 10 μM D-[³H]serine (*A*), L-[³H]serine (*B*), L-[¹⁴C]alanine (*C*), L-[³H]threonine (*D*), [³H]glycine (*E*) or L-[³H]glutamate (*F*). (*G* and *H*) Uptake of either 10 μM D-[³H]serine (*G*) or [³H]glycine (*F*) was measured in HBSS supplemented with 14 μM alanine, 36 μM L-serine, 2 μM cysteine, and 18 μM threonine (A,S,C,T). (*I–L*) Amino acid uptake in primary astrocyte cultures from WT and ASCT2-KO mice in HBSS supplemented with 10 μM D-[³H]serine (*I*), L-[³H]serine (*J*), L-[³H]glutamine (*K*), or L-[³H]glutamate (*L*). The results represent the average ± SEM of four to seven experiments with different astroglia preparations. Different from control at ****P* < 0.001, **0.01, and *0.05 (paired two-tailed Student's *t* test). ns, not a significant difference.

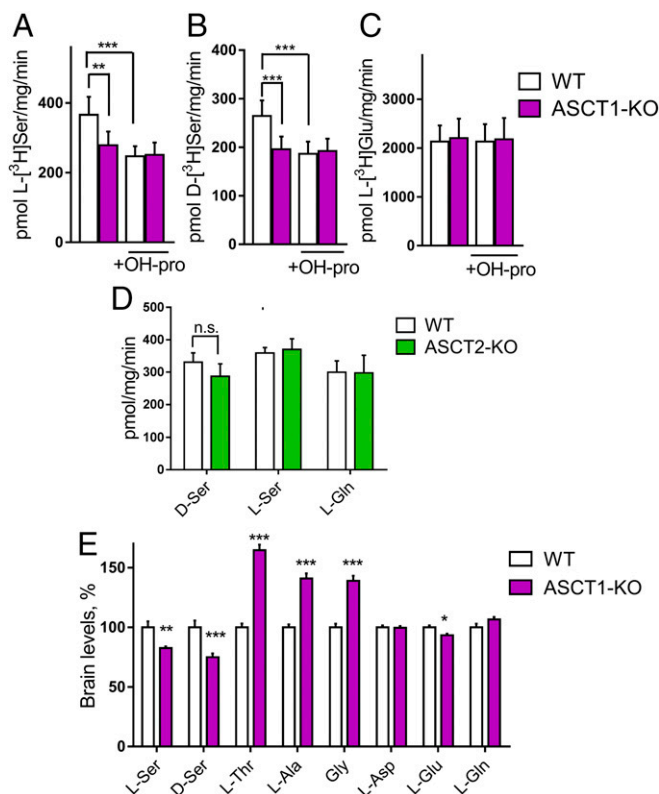


Fig. 2. Amino acid uptake in synaptosomes of ASCT1-KO and ASCT2-KO mice and changes in brain amino acids. (*A–C*) Amino acid uptake in synaptosomes from WT and ASCT1-KO mice monitored in HBSS supplemented with 1 μM D-[³H]serine (*A*), L-[³H]serine (*B*), or L-[³H]glutamate (*C*) either in the absence or in the presence of 1 mM OH-Pro. (*D*) Amino acid uptake in synaptosomes of WT and ASCT2-KO mice. (*E*) Amino acid levels in whole brains of P4 WT (*n* = 10) and ASCT1-KO (*n* = 11) mice. The results represent the average ± SEM of four (*A* and *B*), five (*D*), and seven (*C*) experiments with different preparations. Different from control at ****P* < 0.001, **0.01 and *0.05. n.s., not a significant difference. Repeated measures one-way ANOVA followed by Tukey's post hoc test (*A–C*) or two-tailed Student's *t* test (*D* and *E*).

In cortical synaptosomes, consisting of a mixture of neuronal and glial particles, we detected 30% lower uptake of L-serine and D-serine in preparations from ASCT1-KO mice (Fig. 2 *A* and *B*), a percentage that represents the estimated glial contamination in the synaptosomal preparation (14). We also monitored the effect of *trans*-4-hydroxy-L-proline (OH-Pro), a selective ASCT1 substrate that competes with other substrates (15). In agreement, OH-Pro inhibited the uptake of D-serine transport in HEK293 transfected with ASCT1 to the same extent as excess L-alanine (*SI Appendix, Fig. S2A*). OH-Pro was without effect on ASCT2 or the D-serine transporter Asc-1 (*SI Appendix, Fig. S2 B and C*). OH-Pro inhibited the uptake of D-serine (Fig. 2*B*) and L-serine (Fig. 2*C*) in WT synaptosomes but was without effect on preparations from ASCT1-KO. In contrast with ASCT1, the uptake of typical ASCT2 substrates (e.g., glutamine, L-serine, and D-serine) was unaffected in synaptosomes prepared from ASCT2-KO mice (Fig. 2*D*).

Brain Amino Acids in ASCT1-KO Mice. We measured the levels of ASCT1 and ASCT2 substrates in the brains of their respective KO mice and WT littermates at different ages. Brains from 4-d-old (P4) ASCT1-KO mice exhibited a 20 and 25% decrease in L- and D-serine levels, respectively (Fig. 2*E*). The levels of glycine, L-threonine, and L-alanine were 60–40% higher in ASCT1-KO than in WT mice (Fig. 2*E*). A small 7% decrease in brain L-glutamate was also detected in ASCT1-KO mice. It is noteworthy

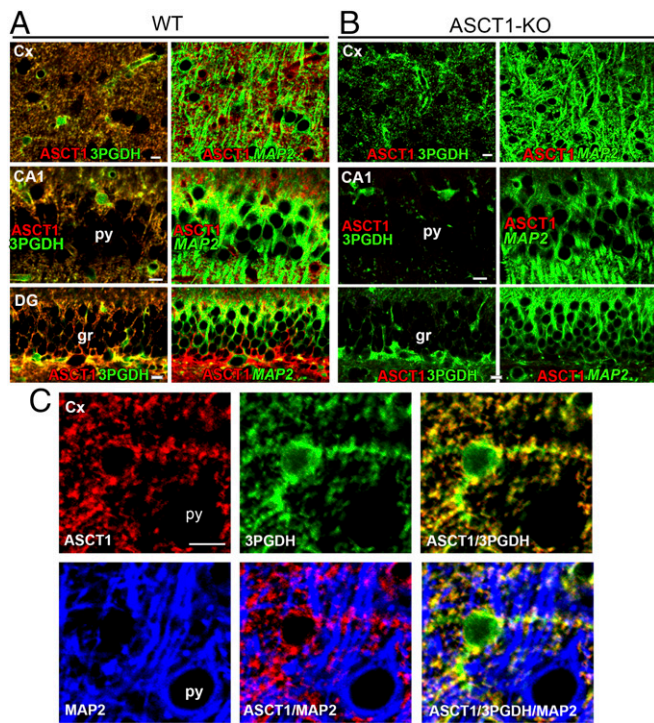


Fig. 3. Astroglial localization of ASCT1 in adult mice. (A) ASCT1 protein (red) colocalizes with the astrocytic marker 3PGDH (green) in WT mice but not with neuronal marker microtubule-associated protein 2 (MAP2). (B) Lack of ASCT1 immunoreactivity in ASCT1-KO mice. (C) High magnification of a cortical astrocyte showing punctuated immunoreactivity for ASCT1 that colocalizes with 3PGDH but is absent from MAP2-expressing cells. CA1, CA1 subfield of the hippocampus; Cx, neocortex; DG, dentate gyrus; gr, granule cells; py, pyramidal cell. (Scale bars, 10 μ m.)

that the ratio between the two NMDAR coagonists (glycine/D-serine) in ASCT1-KO mice brains was almost twice that in WT mice (1.9-fold increase, $P < 0.001$, unpaired Student's t test), indicating a significant increase in total brain glycine relative to D-serine.

Serum levels of L-threonine in P4 ASCT1-KO mice pups were twice the values of WT (SI Appendix, Fig. S3D). However, except for this essential amino acid, serum levels of the other amino acids in P4 mice were not correlated with their brain levels (compare Fig. 2E and SI Appendix, Fig. S3D). The decrease in D-serine levels along with the increase in glycine, L-alanine, and threonine persisted in some brain regions of adult ASCT1-KO mice (SI Appendix, Fig. S3A–C), whereas their serum amino acids were unchanged (SI Appendix, Fig. S3E). Therefore, the developmental changes in brain amino acids observed in ASCT1-KO mice are due to intrinsic changes in brain metabolism unrelated to the levels of serum amino acids.

The levels of different L-serine-derived sphingolipids in the cerebral cortex and striatum were unaltered in ASCT1-KO mice (SI Appendix, Fig. S3F and G), suggesting that the supply of L-serine to lipid synthesis was largely unaffected in adult mice.

However, ASCT2-KO mice had normal levels of brain amino acids (SI Appendix, Fig. S4), further indicating this transporter does not affect mouse brain amino acid metabolism under normal conditions. Therefore, in the subsequent experiments, we focused on investigating the role of its paralog ASCT1.

Astroglial Localizations of ASCT1. ASCT1 expression has been demonstrated either in astrocytes (16) or predominantly in neurons (17). To determine the localizations of ASCT1, we carried out immunohistochemistry using ASCT1-KO mice as negative controls to ensure antibody specificity. We found that ASCT1 colocalizes with the astrocytic marker 3PGDH in the

cerebral cortex, hippocampal CA1 region, and dentate gyrus (Fig. 3A). Immunofluorescence was abolished in ASCT1-KO mice (Fig. 3B). Triple immunofluorescence experiments showed lack of colocalization of ASCT1 with cells expressing the neuronal marker MAP2 (Fig. 3C). At high magnification, punctuated ASCT1 immunoreactivity is observed at the cell bodies and astroglial processes, where it colocalizes with 3PHGDH (Fig. 3C). The data indicate ASCT1 is mainly an astrocytic transporter in adult mice.

Neurodevelopmental Role of ASCT1. Mutations in ASCT1 cause microcephaly in humans (18, 19). Using MRI we found a significant decrease in the volumes of the hippocampus and striatum of ASCT1-KO mice, indicating that they recapitulate some of the alterations seen in humans (Fig. 4). The results of the semiautomated analysis were confirmed by manual analysis of the hippocampus (SI Appendix, Fig. S5). No differences in volumes were observed at the neocortex, cerebellar cortex, and whole brain (Fig. 4B).

We next carried out RNA sequencing of the striatum, which was altered in MRI analysis, and compared it with the neocortex, which was unaffected. We found significant changes in 375 transcripts in the striatum of adult mice at adjusted P values lower than 0.05 (Fig. 4C and Dataset S1). No changes in gene expression were observed in the neocortex (Fig. 4D). In the striatum, enrichment analysis using nonredundant reciprocal linkage of genes identified 11 metagroups, with overrepresentation of genes linked to axonal guidance and neurodevelopment (Fig. 4E and Dataset S2). All metagroups had silhouette width >0.5 (Dataset S2), indicating a high degree of the internal tightness and distance from other metagroups (20). The most significant changes were seen in axon guidance genes (Fig. 4E), suggesting changes in neurodevelopment-related gene transcripts in ASCT1-KO mice.

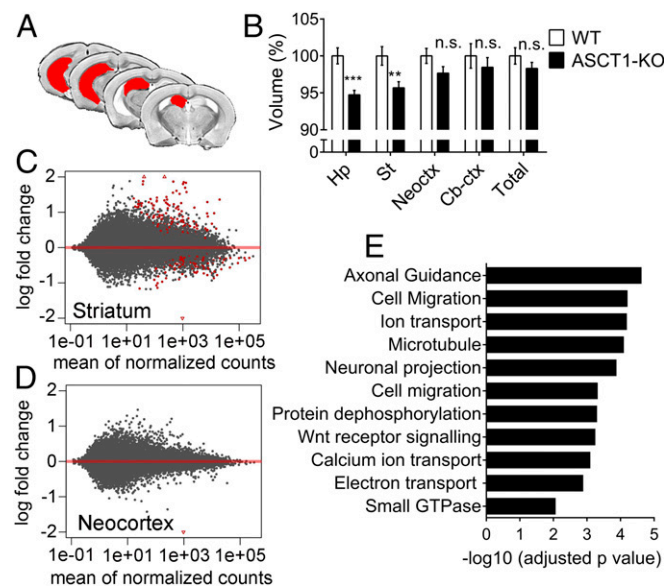


Fig. 4. Brain region volumes and gene expression in ASCT1-KO mice. (A) Hippocampus masking (red) on an average of WT population MRI scans. (B) Total brain and subregions volumes of 9- to 11-month age-matched WT ($n = 12$) and ASCT1-KO ($n = 12$) mice. (C and D) Plots of the delta difference (Log₂) in gene expression between WT and ASCT1-KO mice (y axis) and mean normalized counts (x axis) generated in the striatum and neocortex. Differentially expressed genes are depicted in red symbols. (E) Enrichment analysis in metagroups of differentially expressed genes in the striatum of WT and ASCT1-KO mice according to Gene Ontology biological processes analyzed by nonredundant reciprocal linkage of genes and biological terms. y axis depicts adjusted P values. Different from control at *** $P < 0.001$ and ** $P < 0.01$. n.s., not a significant difference. Unpaired two-tailed Student's t test (B).

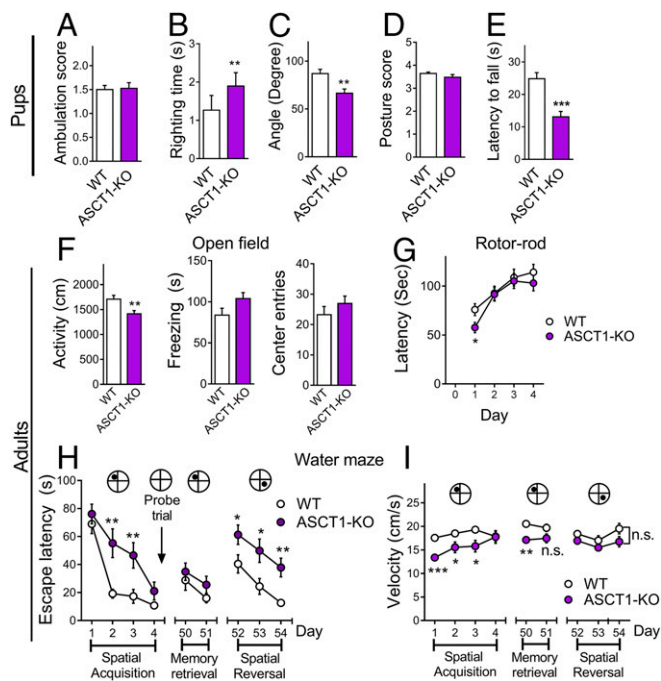


Fig. 5. Behavioral characterization of ASCT1-KO mice. (A) Ambulation scores of P8 WT ($n = 42$) and ASCT1-KO ($n = 19$) mice pups. (B) Righting time showing longer time latency in ASCT1-KO ($n = 19$) compared with WT ($n = 42$) P8 mice (** $P < 0.01$). (C) ASCT1-KO mice ($n = 19$) display weaker grip than WT ($n = 23$) P8 mice (** $P < 0.01$). (D) Hindlimb hanging scores of ASCT1-KO ($n = 19$) and WT ($n = 42$) P8 mice. (E) ASCT1-KO mice ($n = 19$) display shorter latency to fall in the hindlimb suspension test compared with WT ($n = 42$) P8 mice (*** $P < 0.001$). (F) Reduced open-field activity of 4-mo-old ASCT1-KO mice (** $P < 0.01$). (G) Rotor-rod performance of WT and ASCT1-KO mice (* $P < 0.05$). (H) In the Morris water maze task, ASCT1-KO mice reached the platform after longer periods of time on days 2 and 3 (** $P < 0.01$) but attained the same performance as WT at day 4. Memory retrieval by returning the platform and exposing the mice to the same context at days 50 and 51 show identical performance between WT and ASCT1-KO mice. Spatial reversal carried out at days 52–54 revealed significant longer latency in the ASCT1-KO mice (* $P < 0.05$, ** $P < 0.01$). (I) ASCT1-KO mice displayed slower swimming in the first 3 d of the spatial acquisition phase, but not during spatial reversal (* $P < 0.05$, ** $P < 0.01$, *** $P < 0.001$). Experimental groups in F–I consisted of 4- to 5-mo age-matched male mice (12 mice in each group). (A–E) Two-tailed Mann–Whitney U test; (F–I) unpaired two-tailed Student's t test.

Behavioral Changes in ASCT1-KO Mice. We monitored the motor function of mice pups at P8 to evaluate early dysfunction. The ambulation pattern of ASCT1-KO mice was the same as that of WT mice, both exhibiting slow crawling and some asymmetric limb movements (Fig. 5A). However, ASCT1-KO mice exhibited delayed righting response when placed on their backs (Fig. 5B). When placed on an iron mesh that was gradually inverted, ASCT1-KO mice fell at lower angles, suggesting weaker grip strength in the four limbs (Fig. 5C). When suspended by their hind legs at the rim of a conical tube, ASCT1-KO mice pups displayed normal posture (Fig. 5D) but exhibited a shorter latency to fall, suggesting weaker hindlimb strength (Fig. 5E).

Adult ASCT1-KO mice display some degree of motor dysfunction along with impairments in learning and affective domain. Adult ASCT1-KO mice exhibited lower activity in the open field but no significant changes in freezing time or center entries (Fig. 5F). ASCT1-KO mice had a 25% lower latency to fall off the rotor rod on the first day, indicating slightly impaired sensorimotor coordination, although they reached the same latency of the WT in subsequent tests (Fig. 5G). In spatial learning using a Morris water maze, it took ASCT1-KO mice longer to learn the platform location (Fig. 5H, spatial acquisition).

However, once formed, the retention of the spatial memory in ASCT1-KO was the same as in WT mice as observed in the probe trial (SI Appendix, Fig. S6A and B) and memory retrieval test (Fig. 5H). However, ASCT1-KO mice were significantly impaired in spatial learning reversal when the platform location was changed (Fig. 5H, spatial reversal), indicating impairments in learning flexibility. The swimming speed of adult ASCT1-KO mice was 25% slower than WT, indicating possible motor impairment (Fig. 5I). However, the lower swimming velocity per se does not explain the learning deficits. On day 1, despite the difference in swimming speeds, WT and ASCT1-KO mice reached the escape platform after similar delay (Fig. 5H and I). Furthermore, the swimming performance of ASCT1-KO mice improved with subsequent trials and was identical to that of WT during the spatial reversal test (Fig. 5I).

Amygdala-dependent fear learning monitored by the active two-way avoidance test was normal in ASCT1-KO mice (SI Appendix, Fig. S6C). ASCT1-KO mice displayed a 60% increase in startle response, known to be enhanced in anxiety (SI Appendix, Fig. S6D). However, the ASCT1-KO mice did not exhibit changes in prepulse inhibition (SI Appendix, Fig. S6E), indicating an intact sensorimotor gating. A sucrose preference test showed decreased preference at 72 h (SI Appendix, Fig. S6F) but normal fluid intake (SI Appendix, Fig. S6G).

Synaptic Activity in ASCT1-KO Mice. The long-term potentiation (LTP) at the Schaffer collateral-CA1 synapses of the hippocampus was normal in ASCT1-KO mice (SI Appendix, Fig. S7A). LTP in WT animals was unchanged by the addition of the ASCT1 substrate OH-Pro (SI Appendix, Fig. S7B). The long-term depression induced by low-frequency stimulation was normal in ASCT1-KO mice (SI Appendix, Fig. S7C). No changes were detected in basal neurotransmission or isolated NMDAR potentials (SI Appendix, Fig. S7D and E).

In light of their normal NMDAR activity, we wondered if the higher levels of brain glycine in ASCT1-KO mice might compensate for the decrease in D-serine (Fig. 2E and SI Appendix, Fig. S3A–C). To investigate this possibility, we treated hippocampal slices of WT and ASCT1-KO mice with glycine oxidase enzyme (GO) to remove glycine (6). To increase the sensitivity of the method, we employed six- to sevenfold lower GO (in activity units) than in previous reports (6, 21). The use of a limiting amount of GO allows only partial removal of endogenous glycine. Under this condition, GO treatment will likely be less effective in samples displaying higher glycine levels or increased glycine release. We found that treatment with low GO titer decreased the expression of the NMDAR-dependent LTP from WT mice by almost 50% (SI Appendix, Fig. S7F). LTP in slices from ASCT1-KO mice were unaffected by the treatment with low GO titer (SI Appendix, Fig. S7G), suggesting their higher glycine levels might surpass the GO enzymatic capacity. In addition, we also monitored the effect of the glycine transporter 1 inhibitor ALX 5407, known to increase synaptic glycine (1). ALX 5407 augmented the isolated NMDAR potentials of both WT and ASCT1-KO mice (SI Appendix, Fig. S7H). However, the extent of stimulation by ALX 5407 was slightly lower in slices from ASCT1-KO mice compared with WT controls (SI Appendix, Fig. S7H), indicating that NMDARs from ASCT1-KO may be slightly more saturated with glycine. We also examined place cells in the CA1 region of mice by in vivo electrophysiology, which showed their activity is preserved in ASCT1-KO mice, excluding significant changes (SI Appendix, Fig. S8).

Amino Acid Exchange by ASCT1 in Vitro and in Vivo. To investigate the ability of ASCT1 in releasing endogenous amino acids, we investigated the effects of OH-Pro in acute cortical slices. As a selective ASCT1 substrate, it is expected that OH-Pro will exchange with intracellular ASCT1 substrates. Perfusion with OH-Pro elicited release of L-serine in slices of WT mice but did not affect the release of L-serine in slices of ASCT1-KO mice (Fig. 6A). Endogenous L-alanine and L-threonine were also released

by OH-Pro in acute slices (Fig. 6B and C). Although D-serine is a bona fide ASCT1 substrate for uptake, addition of OH-Pro did not elicit the release of endogenous D-serine, indicating D-serine is preferentially taken up via ASCT1 (Fig. 6D). Likewise, OH-Pro did not elicit detectable release of glycine (Fig. 6E).

We subsequently monitored the extracellular concentrations of typical ASCT1 substrates by in vivo microdialysis of the striatum. Values were corrected by the in vivo recovery through infusion of stable-isotope-labeled amino acids (22). ASCT1-KO mice displayed a 25% decrease in the steady-state extracellular levels of D-serine, with no change in the extracellular L-serine levels (Fig. 6F and G). In addition, ASCT1-KO mice exhibited a decrease in the ratio of extracellular D-serine/total serine (Fig. 6H). We found no change in the extracellular concentrations of alanine, threonine, and glycine in adult ASCT1-KO mice (Fig. 6I–K).

Discussion

We identified ASCT1 as an important D- and L-serine transporter in astrocytes and a potential player in the serine shuttle between glia and neurons (Fig. 6L). ASCT1 is an obligatory exchanger that displays faster kinetics than unidirectional amino acid transporters (12). Its exchange activity will likely facilitate reaching a steady-state concentration gradient across the membrane by increasing the rates of transport of its substrates. This is in agreement with our observations in primary astrocyte cultures, synaptosomes, and acute brain slices. Our in vivo microdialysis data, however, indicate that ASCT1 does not alter the absolute extracellular amino acid concentrations at steady state, except for D-serine. Extracellular levels of D-serine were 25% lower in the striatum of ASCT1-KO mice (Fig. 6G). The decrease in extracellular D-serine is in agreement with the lower levels of total brain D-serine in young and adult ASCT1-KO mice (Fig. 2 and *SI Appendix*, Fig. S3A–C).

We propose that ASCT1 carries out bidirectional transport of all its neutral amino acid substrates but D-serine (Fig. 6L). Although ASCT1 catalyzes the release of previously loaded D-³H]serine from cells (11), activation of ASCT1 heteroexchange by OH-Pro in acute cortical slices did not release endogenous D-serine. This result is in agreement with previous studies demonstrating much lower levels of endogenous D-serine in astrocytes compared with neurons (5, 7–10). Conceivably, the low amounts of D-serine in the cytosol of astrocytes fall below the affinity of the ASCT1.

The decrease in both the total and the extracellular levels of D-serine observed in ASCT1-KO mice suggests a partial impairment in brain D-serine production. L-serine made in astrocytes appears to shuttle to neurons to fuel the synthesis of D-serine in a process called the serine shuttle (Fig. 6L) (10). Even though extracellular L-serine was unchanged in adult ASCT1-KO mice, our observations that ASCT1-KO mice are deficient in L-serine transport imply that the equilibrative nature of the ASCT1 transporter is required to provide enough L-serine for D-serine synthesis in the local contacts between astrocytes and neurons (Fig. 6L). Further evidence supporting a role of ASCT1 in the serine shuttle comes from our findings demonstrating a significant decrease in both L-serine and D-serine in brains from ASCT1-KO P4 mice (Fig. 2E). However, in vivo microdialysis was impractical in P4 mice pups, where changes in L-serine and other ASCT1 substrates were more prominent than in adult mice (compare Fig. 2E and *SI Appendix*, Fig. S3). Our data, however, do not exclude that other L-serine transporters may partially compensate for the lack of ASCT1 in the KO mice. Other components of the serine shuttle, such as the neuronal uptake system for L-serine, still remain to be identified.

In contrast to D-serine, levels of L-serine-derived sphingolipids were normal in ASCT1-KO mice. This might be due to the high-affinity exhibited by the serine palmitoyltransferase (SPT), the key enzyme for sphingolipid biosynthesis. SPT has a 30-fold higher affinity for L-serine ($K_m \sim 0.3$ mM) (23) compared with the D-serine biosynthetic enzyme, SR ($K_m \sim 10$ mM) (10). Therefore,

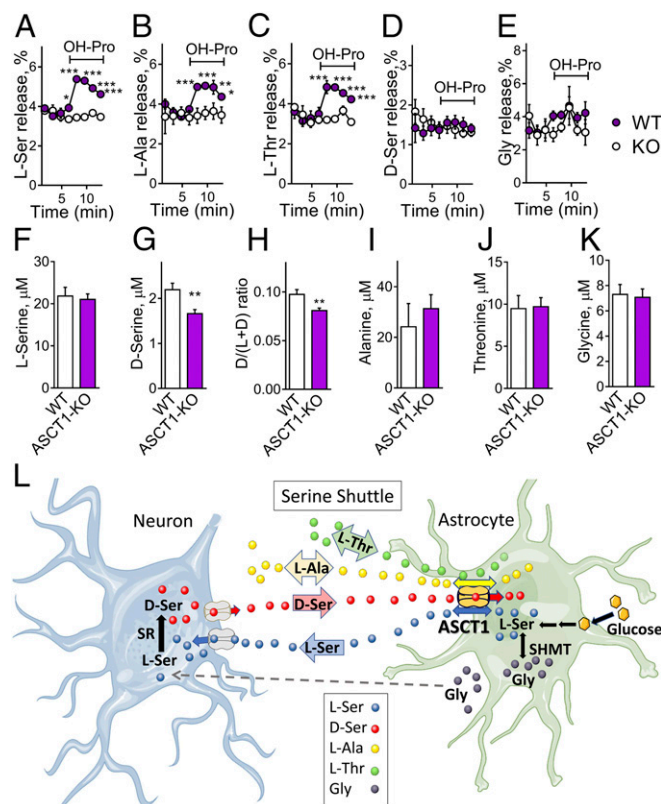


Fig. 6. ASCT1-mediated amino acid exchange in slices and in vivo microdialysis. (A–E) Release of endogenous L-serine (A), L-alanine (B), L-threonine (C), D-serine (D), and glycine (E) was elicited by perfusion of slices with 1 mM OH-pro at the indicated times. The data are average \pm SEM of seven experiments. Different from ASCT1-KO mice at $*P < 0.05$ and $***P < 0.001$ (two-way repeated measures ANOVA and Bonferroni's post hoc test). (F–K) Extracellular amino acid concentrations in the striatum of 6- to 7-month-old mice by in vivo microdialysis (12 mice per group). The data represent the mean \pm SEM of the extracellular amino acid concentrations calibrated by the recovery in vivo. $**$ Different from WT at $P < 0.01$, unpaired two-tailed Student's *t* test. (L) Proposed model of ASCT1 function in the serine shuttle. Astrocytic ASCT1 releases L-serine, which is subsequently taken up by neurons to fuel the synthesis of D-serine by the SR. D-serine may be released by neurons via the Asc-1 (Slc7a10) transporter (26) and subsequently taken up by ASCT1 in astrocytes. L-alanine, L-threonine, and D-serine may serve as extracellular substrates that stimulate L-serine export via ASCT1 by heteroexchange. Impairment in L-serine transport in ASCT1-KO mice may lead to increased conversion of L-serine into glycine by the serine hydroxymethyl transferase (SHMT) enzyme. When the serine shuttle is impaired, glycine taken up by neurons (dashed arrow) may provide a compensatory pathway for supplying L-serine to neurons via neuronal SHMT. Adapted with permission from Servier Medical Art, <https://smart.servier.com/>.

the low affinity of SR for L-serine makes the D-serine synthesis particularly sensitive to impairments in the serine shuttle.

Our study also uncovers the role of ASCT1 in alanine, threonine, and glycine metabolism, as their total brain levels increased in ASCT1-KO mice. Astrocytes are known to carry out the metabolism of alanine into lactate (24), whereas threonine is an essential amino acid that reaches the brain via the blood-brain barrier. Conceivably, deficient alanine and threonine transport in ASCT1-KO mice will partially impair their metabolism in astrocytes and lead to their accumulation. However, glycine is a poor ASCT1 substrate (Fig. 1H). Higher levels of glycine in ASCT1-KO mice may be a consequence of L-serine transport impairment. Deficient exchange of L-serine in ASCT1-KO astrocytes may favor L-serine conversion into glycine by the serine hydroxymethyl transferase enzyme (Fig. 6L).

Interestingly, our results using both enzymatic removal of endogenous glycine and a glycine transport inhibitor suggest higher occupancy of NMDARs by glycine in ASCT1-KO mice. Since glycine is also a regulator of synaptic NMDARs (4, 11, 21), higher glycine occupancy might help to preserve NMDAR, as we found in ASCT1-KO mice. Furthermore, higher brain glycine may provide a compensatory mechanism to overcome impairments in the serine shuttle, as glycine released from astrocytes may be taken up by neurons and subsequently converted into L-serine (Fig. 6L, dotted line). Future studies will be required to clarify the exact role of ASCT1 in alanine, threonine, and glycine metabolism. Our study also does not provide information on the role of ASCT1 in cysteine transport. Although L-cysteine is a substrate for ASCT1 in vitro, almost all extracellular cysteine is present in the form of cystine, which is imported into the cells by a dedicated cystine/glutamate transporter (25).

Our finding of lower striatal and hippocampal volumes in ASCT1-KO mice associated with changes in the expression of neurodevelopment-relevant genes partially recapitulates some of the neurodevelopmental alterations in patients with mutations in ASCT1 transporter (18, 19). We found that ASCT1-KO mice also display motor impairments and behavioral deficits in learning and affective tests. ASCT1-KO mice exhibited impaired spatial learning in the Morris water maze, which cannot be solely explained by their lower swimming speed. Although the ASCT1-KO mice displayed smaller hippocampal volumes, extensive *ex vivo* and *in vivo* electrophysiology did not unveil hippocampal dysfunction under our recording conditions. It is likely that the combined impairments of motor function (e.g., lower swimming velocity, open field activity, and latency in the rotor rod) along with changes in the affective behavior (lower sucrose preference and possible anxiety as revealed by higher startle response) may have contributed to the learning impairment in the Morris water maze.

The phenotypic abnormalities of ASCT1-KO mice differ from those exhibited by SR-KO mice, which mostly lack D-serine (3). SR-KO mice have normal motor function, unaltered startle response, and no evidence of impairment in learning acquisition in the Morris water maze. Therefore, the motor and learning abnormalities observed in ASCT1-KO mice likely result from the combination of D-serine deficits with a broader metabolic change in amino acids we described here, including alanine, threonine, and glycine. In this framework, ASCT1-KO mice will be useful for

developing therapeutic interventions to prevent or reduce the neurodevelopmental deficits in patients with mutations in ASCT1.

Materials and Methods

Animals. Slc1a4^{tm1e(KOMP)Wtsi} mice (ASCT1-KO) were obtained from Sanger Institute on a C57BL/6N genetic background. Slc1a5 KO mice (ASCT2-KO) were obtained from Taconic and back-crossed in our facility with C57BL/6J mice for 10 generations. All animal procedures were in accordance with the Committee for the Supervision of Animal Experiments (Technion – Israel Institute of Technology).

Western Blots. The brains were homogenized in buffer containing 20 mM Tris-HCl (pH 7.4), 100 mM NaCl, 0.4 mM PMSF, and 1 mM EDTA. The homogenate was centrifuged at 1,500 × *g* for 10 min and the supernatant was collected and then centrifuged at 200,000 × *g* for 30 min. The pellet, containing the membrane fraction, was subjected to SDS/PAGE followed by Western blot. For ASCT2 western blot, the samples were first deglycosylated by adding 1,000 units of PNGase F under nonreducing conditions according to the manufacturer's instructions (New England Biolabs). To minimize the aggregation of membrane proteins, the samples were not boiled after addition of sample buffer containing SDS.

Amino Acid Uptake in Cell Cultures. Primary astrocyte cultures were obtained from the cortices of P0–P2 mice as previously described (11) and used 12–14 d after plating. For uptake experiments, cultures were incubated in 96-well plates for 5–7 min with 1 μM [³H]amino acids in Hepes-buffered saline (HBS, in millimolar: 137 NaCl, 5.4 KCl, 0.18 Na₂HPO₄, 0.44 KH₂PO₄, 0.41 MgSO₄, 0.49 MgCl₂, 1.07 CaCl₂, 5.6 D-glucose, 4.2 NaHCO₃, 1 Na-pyruvate, and 10 Hepes, pH 7.4) at 25 °C. The [³H]amino acid transport was terminated by washing the cells four times with ice-cold HBS and processed as previously described (11).

Additional methods are described in *SI Appendix, Supplemental Methods*.

ACKNOWLEDGMENTS. We thank O. Schwartz and Dr. E. Suss-Toby (BCF Bioimaging Center, Faculty of Medicine, Technion) for the MRI; Dr. Itamar Khan for guidance and supervision in MRI analysis; and Drs. Liat Linde, Dr. Ronit Modai-Hod, Elizabeta Ginzburg, and Doron Fogel (BCF Genomics Center, Faculty of Medicine, Technion) for RNA sequencing. This work was funded by the Israel Science Foundation (H.W.) and the Vivian and Oscar Lasko fund for Parkinson's and Alzheimer Research (H.W.), the Allen and Jewell Prince Center for Neurodegenerative Disorders of the Brain (H.W., D.D., and A.A.), and Michigan-Israel Partnership for Research and Education funds (H.W. and R.T.K.). J.-M.B. was supported by the Institut National de la Santé et de la Recherche Scientifique. T.Y.'s research was supported by Japan Agency for Medical Research and Development (AMED) under Grant JP18dm0107083, AMED-Core Research for Evolutional Science and Technology under Grant JP18gm0910004, and Ministry of Education, Culture, Sports, Science and Technology under Grant JP18H05435.

- Traynelis SF, et al. (2010) Glutamate receptor ion channels: Structure, regulation, and function. *Pharmacol Rev* 62:405–496.
- Wolosker H, Blackshaw S, Snyder SH (1999) Serine racemase: A glial enzyme synthesizing D-serine to regulate glutamate-N-methyl-D-aspartate neurotransmission. *Proc Natl Acad Sci USA* 96:13409–13414.
- Basu AC, et al. (2009) Targeted disruption of serine racemase affects glutamatergic neurotransmission and behavior. *Mol Psychiatry* 14:719–727.
- Li Y, et al. (2013) Identity of endogenous NMDAR glycine site agonist in amygdala is determined by synaptic activity level. *Nat Commun* 4:1760.
- Perez EJ, et al. (2017) Enhanced astrocytic D-serine underlies synaptic damage after traumatic brain injury. *J Clin Invest* 127:3114–3125.
- Panatier A, et al. (2006) Glia-derived D-serine controls NMDA receptor activity and synaptic memory. *Cell* 125:775–784.
- Balu DT, Takagi S, Puhl MD, Benneworth MA, Coyle JT (2014) D-serine and serine racemase are localized to neurons in the adult mouse and human forebrain. *Cell Mol Neurobiol* 34:419–435.
- Ehmsen JT, et al. (2013) D-serine in glia and neurons derives from 3-phosphoglycerate dehydrogenase. *J Neurosci* 33:12464–12469.
- Wolosker H, Balu DT, Coyle JT (2016) The rise and fall of the D-serine-mediated gliotransmission hypothesis. *Trends Neurosci* 39:712–721.
- Wolosker H, Radziszewsky I (2013) The serine shuttle between glia and neurons: Implications for neurotransmission and neurodegeneration. *Biochem Soc Trans* 41:1546–1550.
- Rosenberg D, et al. (2013) Neuronal D-serine and glycine release via the Asc-1 transporter regulates NMDA receptor-dependent synaptic activity. *J Neurosci* 33:3533–3544.
- Bröer S, Bröer A (2017) Amino acid homeostasis and signalling in mammalian cells and organisms. *Biochem J* 474:1935–1963.
- Lindroth P, Hamberger A, Sandberger M (1985) Liquid chromatography determination of amino acids after precolumn fluorescent derivatization. *Amino Acids (Neuromethods)*, eds Boulton AA, Baker GB, Wood JD (Humana, Clifton, NJ), 1st Ed, Vol 3, pp 97–116.
- Henn FA, Anderson DJ, Rustad DG (1976) Glial contamination of synaptosomal fractions. *Brain Res* 101:341–344.
- Foster AC, et al. (2017) Phenyglycine analogs are inhibitors of the neutral amino acid transporters ASCT1 and ASCT2 and enhance NMDA receptor-mediated LTP in rat visual cortex slices. *Neuropharmacology* 126:70–83.
- Sakai K, Shimizu H, Koike T, Furuya S, Watanabe M (2003) Neutral amino acid transporter ASCT1 is preferentially expressed in L-Ser-synthetic/storing glial cells in the mouse brain with transient expression in developing capillaries. *J Neurosci* 23:550–560.
- Weiss MD, Derazi S, Kilberg MS, Anderson KJ (2001) Ontogeny and localization of the neutral amino acid transporter ASCT1 in rat brain. *Brain Res Dev Brain Res* 130:183–190.
- Heimer G, et al. (2015) SLC1A4 mutations cause a novel disorder of intellectual disability, progressive microcephaly, spasticity and thin corpus callosum. *Clin Genet* 88:327–335.
- Damseh N, et al. (2015) Mutations in SLC1A4, encoding the brain serine transporter, are associated with developmental delay, microcephaly and hypomyelination. *J Med Genet* 52:541–547.
- Fontanillo C, Nogales-Cadenas R, Pascual-Montano A, De las Rivas J (2011) Functional analysis beyond enrichment: Non-redundant reciprocal linkage of genes and biological terms. *PLoS One* 6:e24289.
- Le Bail M, et al. (2015) Identity of the NMDA receptor coagonist is synapse specific and developmentally regulated in the hippocampus. *Proc Natl Acad Sci USA* 112: E204–E213.
- Hershey ND, Kennedy RT (2013) In vivo calibration of microdialysis using infusion of stable-isotope labeled neurotransmitters. *ACS Chem Neurosci* 4:729–736.
- Hanada K, Hara T, Nishijima M (2000) Purification of the serine palmitoyltransferase complex responsible for sphingoid base synthesis by using affinity peptide chromatography techniques. *J Biol Chem* 275:8409–8415.
- Waagepetersen HS, Sonnewald U, Larsson OM, Schousboe A (2000) A possible role of alanine for ammonia transfer between astrocytes and glutamatergic neurons. *J Neurochem* 75:471–479.
- Warr O, Takahashi M, Attwell D (1999) Modulation of extracellular glutamate concentration in rat brain slices by cystine-glutamate exchange. *J Physiol* 514:783–793.
- Sason H, et al. (2017) Asc-1 transporter regulation of synaptic activity via the tonic release of D-serine in the forebrain. *Cereb Cortex* 27:1573–1587.